



Published in final edited form as:

*Chemistry*. 2010 March 22; 16(12): 3791–3797. doi:10.1002/chem.200901546.

## DNA Based Micelles: Synthesis, Micellar Properties and Size-dependent Cell Permeability

**Dr. Haipeng Liu, Zhi Zhu, Huaizhi Kang, Yanrong Wu, Kwame Sefan, and Prof. Weihong Tan**

Center for research at the Bio/Nano Interface, Department of Chemistry Shands Cancer Center, UF Genetics Institute and McKnight Brain Institute, University of Florida, Gainesville, Florida 32611-7200, USA, Fax: (+1) 352-846-2410

Weihong Tan: tan@chem.ufl.edu

### Abstract

Functional nanomaterials based on molecular self-assembly hold great promise for applications in biomedicine and biotechnology. However, their efficacy could be a problem and can be improved by precisely controlling the size, structure and functions. This would require a molecular engineering design capable of producing monodispersed functional materials characterized by beneficial changes in size, shape and chemical structure. To address this challenge, we have designed and constructed a series of amphiphilic oligonucleotide molecules. In aqueous solutions, the amphiphilic oligonucleotide molecules, consisting of a hydrophilic oligonucleotide covalently linked to hydrophobic diacyllipid tails, spontaneously self-assemble into monodispersed, three dimensional micellar nanostructures with a lipid core and a DNA corona. These hierarchical architectures are results of intermolecular hydrophobic interactions. Experimental testing further showed that these types of micelles have excellent thermal stability and their size can be fine tuned by changing the length of the DNA sequence. Moreover, in the micelle system, the molecular recognition properties of DNA are intact, thus, our DNA micelles can hybridize with complimentary sequences while remain their structural integrity. Importantly, when interacting with cell membranes, the highly charged DNA micelles are able to disintegrate themselves and insert into cell membrane, completing the process of internalization by endocytosis. Interestingly, the fluorescence was found accumulated in confined regions of cytosole. Finally, we show that the kinetics of this internalization process is size-dependent. Therefore, cell permeability, combined with small sizes and natural nontoxicity, are all excellent features that make our DNA-micelles highly suitable for a variety of applications in nanobiotechnology, cell biology, and drug delivery systems.

### Keywords

DNA; Micelles; Amphiphilic; Self-assemble; Cell permeability

### Introduction

The increasing attention given to the construction of complex supramolecular structures from simple amphiphilic molecules via molecular self-assembly can be attributed to their broad spectrum of applications, ranging from molecular electronics to biomedicine.<sup>[1–4]</sup> Amphiphilic peptides,<sup>[1]</sup> nucleic acids,<sup>[2]</sup> lipids<sup>[3]</sup> and polymers<sup>[4]</sup> have been shown to generate ordered supramolecular structures such as monolayers, micelles, vesicles, bilayers

and nanotubes. For biomedical applications, micelle structures are of particular interest because of their small size, good biocompatibility, high stability both in vitro and in vivo, and the ability to carry poorly soluble pharmaceuticals into intracellular regions.

The ability to produce supramolecular assemblies with accurate control over their composition, structure and function on the nanometer scale is highly desired. Recently, micellar aggregates that are composed of a single-stranded DNA corona and a hydrophobic polymer core have emerged as new types of functional micelles.<sup>[2]</sup> These micelles have been synthesized and applied for the delivery of antisense DNA,<sup>[2a]</sup> as 3-D scaffold for organic reactions,<sup>[2f]</sup> and as a combinatorial tool for cancer nanotechnology.<sup>[2g]</sup> While a variety of DNA-micelle systems have been demonstrated,<sup>[2]</sup> the coupling between synthetic DNA and hydrophobic tail has often been inefficient; in some cases, an extra purification process, such as PAGE or agarose gel electrophoresis, is needed. More important, the size of the self-assembly is usually not well-controlled, as the polymer has wide molecular weight distribution.<sup>[2c]</sup> A uniform size distribution is favoured over a broad distribution because of the unpredictable change of micelles' pharmacokinetic parameters. Apparently, the design and construction of well-defined micelle systems is central to the development of nanobiotechnological applications. However, achieving this goal demands precise molecular engineering of the corresponding building blocks, since all the information required for the assembly must be encoded in its molecular architecture. To date, studies describing the construction of such well-defined oligonucleotide-micelle structures are scarce.<sup>[1b]</sup> In addition, the detailed structure-property characterization of DNA- micelles has not been reported. The present study, which addresses both gaps in our knowledge, reports the design and construction of a well-defined DNA-micelle system through a DNA-diacyllipid conjugate. We show that a diacyllipid tail can be efficiently incorporated at the 5' end of oligonucleotides by solid phase DNA synthesis. When dispersed in aqueous solution, such amphiphilic DNA spontaneously self-assembled into a monodispersed micelle structure. We investigated the self-assembly properties, including micellar stability, by means of fluorescence techniques, gel electrophoresis, atomic force microscopy (AFM) and dynamic light scattering (DLS). Finally, we demonstrated that these DNA-micelles disintegrate themselves when incubated with biological cells, permeating the cell membrane by a process of endocytosis. Thus, it is additionally interesting to discover that the permeability of our DNA -micelles is size-dependent.

Our oligonucleotide-lipid conjugates have the same basic architecture as phospholipids, but they consist of distinct and highly negatively charged DNA chains covalently linked with two hydrocarbons. We highlight the simple and efficient synthesis and assembly of our DNA micelles. Their unique properties, such as excellent cell permeability, low critical micelle concentration (CMC), and nontoxicity, may lead to their applications in drug delivery and cell biology.

## Results and Discussion

Natural systems are known to self-assemble into complex architectures with structural precision and a high level of control. In an attempt to mimic this process, the ability to control the size, shape and function of the micelle assembly is highly desired. In developing well-defined, stable oligonucleotide supramolecular structure, our attention was therefore directed towards a practical method of conjugating a hydrophobic diacyllipid to DNA. We hypothesized that a precise molecular architecture would ultimately lead to a uniform assembly. Previous DNA-polymer conjugates had suffered low reaction yield, purification difficulties, and broad molecular weight distributions.<sup>[2b, 2c, 2f]</sup> Inspired by recent success in solid phase synthesis of hydrophobic conjugates of oligonucleotides,<sup>[5,6]</sup> we adapted a similar strategy and synthesized a lipid phosphoramidite to meet our design requirements.

Our design is illustrated in Figure 1. The amphiphilic building block can be divided into three distinct segments. The first segment is a single-stranded DNA, which is highly hydrophilic. DNA was chosen as a micelle-forming material because of its well-defined structure as well as its versatile chemical and biological functions. The second segment is a pyrene molecule. Here, a pyrene unit acts as a fluorescence reporter because it has unique fluorescence characteristics which have been widely used to probe the aggregation behaviour of various systems.<sup>[7]</sup> The highly hydrophobic third segment is composed of two C18 hydrocarbon tails. In water, the hydrophobic effect is the driving force for micelle formation. Based on the amphiphilic nature of our design, we hypothesized that the DNA-lipid molecules would be able to self-assemble as a result of hydrophobic effect. In addition, both the size and the function of the micelles can be readily adjusted by fine tuning the sequence of DNA corona. This provides unique control over the construction of nanostructures, which, in turn, results in significant diversity, flexibility and functionality.

Our facile synthesis includes a pyrene and a diacyllipid phosphoramidite. The introduction of phosphoramidite chemistry allows a synthesis of all the components in a fully automated fashion, which greatly increases the reaction yield. The amphiphiles were prepared in moderate yield (estimated 60% lipid coupling yield) through solid phase synthesis on controlled pore glass beads (CPG) (SI, Fig. S1). The lipid coupling was confirmed by mass spectrometry (SI, Fig. S2). Four amphiphiles with different DNA lengths (random sequences, lipo-n, where n denotes the length of oligonucleotides) were prepared and used for the self-assembly. In aqueous solutions, these DNA amphiphiles spontaneously self-assembled into three-dimensional spherical micelles with a DNA corona and a lipid core. The self-assembly characteristics were then investigated by employing fluorescence techniques. In the aggregation state, the pyrene units, which were designed to be close to the lipid tails, are spatially proximate to each other and give excimer-type fluorescence of pyrene.<sup>[8]</sup> All four DNA-micelles used in this study revealed a broad emission of pyrene excimer at 480 nm with an excitation at 350 nm in aqueous solution, as shown by the fluorescent spectra in Figure 2a. This result shows the strong  $\pi$ - $\pi$  excitonic interactions of the pyrene chromophores in the micelle systems, which indicates the well-organized state of the assembled micelles. In addition, when a DNA without lipid (py-20; same sequence as lipo-20, but without lipid coupling) was tested, no excimer fluorescence was observed (Figure 2a, b). Amphiphilic assemblies normally form in response to solvent compositional change. Figure 2b shows images of micelles in different solvent systems. As expected, the micelle structures are disrupted when acetone (a good solvent for lipid) was added as a cosolvent. These results strongly suggest the formation of aggregates when the DNA amphiphiles were dispersed in water. Importantly, the hybridization of the complementary DNA by formation of Watson-Crick base pairs does not seem to affect the aggregation (SI, Fig. S3), which suggests that it is possible to further manipulate these assemblies. Taken together, the fluorescence outcome matches a key objective of our design strategy because it proves our ability to obtain the desired aggregation assemblies. We also noticed that for a effective micelle formation, diacyllipid is crucial. When a monoacyllipid (single C18 hydrocarbon, less hydrophobic) was used, no micelle formed, even at millimolar concentration.

Unlike previously reported DNA-polymer conjugates which have a range of molecular weights and sizes,<sup>[2a, 2c, 2d]</sup> our design has a precise molecular architecture. Therefore, we designed further experiments to test whether our DNA amphiphiles could self-assemble into well-defined, homogeneous micelles. To accomplish this, we conducted agarose gel electrophoresis experiments. Gel electrophoresis is a powerful technique in biology and is the standard method used to separate, identify and purify nucleic acid with different sizes. We hypothesized that micelle aggregation in the gel matrix would result in slow moving bands with green fluorescence (pyrene excimer). On the other hand, if aggregations were to

be disrupted, we further hypothesized that only fast moving bands with violet fluorescence (monomeric pyrene) would be observed. In addition, a sharp or condensed band would be consistent with uniform size and unique conformation. Since the mobility of our DNA amphiphiles solely depended on the length of the DNA, shorter DNA assemblies would generally be expected to migrate faster in the gel. As shown in Figure 2c, in TBE buffer, each DNA assembly migrated as a single, sharp band with expected mobility, suggesting that the micelle aggregations were stably formed. It should be noted that the self-assembled structures exhibited single sharp bands for all of the assemblies, indicating that all the micelles are quite uniform in aggregation number. Nonetheless, attempts to estimate the aggregation number by a reported method<sup>[9]</sup> yielded inconclusive results, which was most likely caused by the interference of the highly charged DNA. To further prove that the slow mobility was a result of aggregation, we added 0.8% (w/v) sodium dodecyl sulfate (SDS) to the gel. At this concentration, SDS can disrupt micelles, resulting in a loss of hydrophobic interactions.<sup>[10]</sup> As expected, under UV illumination, all the DNA migrated as faster single violet (monomeric pyrene) bands (Figure 2d), demonstrating conclusively that the aggregation of DNA micelles was actually a result of the hydrophobic effect caused by the diacyllipid tails.

To provide direct evidence of amphiphilic DNA self-assembly into micelles, we imaged the sample using tapping mode atomic force microscopy (AFM) in PBS buffer. AFM images revealed a dense layer of highly uniform spherical particles (Figure 3a). The morphological characteristics of the DNA micelles under AFM were quite different from those of the synthetic diblock polymer micelles. The height of the micelles, as measured by AFM, was about 1.2 nm, a value about half that of a double-strand DNA measured in liquid.<sup>[11]</sup> However, it is known that strong electrostatic interactions with the substrate and the vertical forces in tapping mode AFM commonly deform soft materials, leading to compressed morphologies.<sup>[12]</sup> Therefore, we used an alternate method, dynamic light scattering (DLS), which provides a fast, direct measurement of the physical sizes, as well as aggregation data for the dissolved DNA micelles (Figure 3). The hydrodynamic diameters in PBS buffer, as measured by DLS, for lipo-5, lipo-10, lipo-20 and lipo-50, were 7.8 nm, 9.5 nm, 14.6 nm and 36.4 nm, respectively. These values agree well with the sizes of micelle aggregations, but they are far less than those in previously reported DNA vesicles.<sup>[2e]</sup> Despite the unknown conformation and persistence data for ssDNA, micelle size that is linearly proportional to DNA length suggests a predictable relationship. We believe the highly uniform sizes of these micelles originate from two sources. First, our precisely engineered molecular building block facilitates the uniform assembly. Second, the highly negatively charged oligonucleotides repel each other and stretch themselves without tangling together.<sup>[13]</sup>

The stability of our DNA-micelles was then investigated. Remarkably, all DNA-micelle solutions had very low critical micelle concentrations (below 10 nM; SI, Fig. S4). Because of the limited fluorescence of pyrene, we note that 10 nM should be considered the upper limit of CMC, rather than the actual values. Nevertheless, these extremely low CMCs indicate excellent stability compared to polymer micelle systems.<sup>[14]</sup> The thermal stability of the DNA-micelles was also investigated. In the presence of counterions (1xPBS buffer, 137mM Na<sup>+</sup>, 2.7mM K<sup>+</sup>), DNA-micelles maintained their integrity (excimer-type fluorescence peak), even at 95°C. When the temperature study was conducted in pure water, however, the excimer-type fluorescence vanished as temperature increased, while the monomeric fluorescence increased its intensity, showing a ratiometric response (SI, Fig. S5). These data indicate that counterions can greatly stabilize the DNA-micelles, most likely by minimizing the anionic charge repulsion between DNA chains. We believe that the unusual stability of our DNA-micelles partially arises from the design itself, where the covalent linkage of two dramatically distinct segments prevents the dissociation and breakup of

hydrophobic interactions. Finally, the micelles are stable for at least 12 months without formation of any precipitation when stored at 4 °C.

DNA derivatives with lipophilic moieties, such as cholesterol,<sup>[15]</sup> dendrimers,<sup>[16]</sup> polymers,<sup>[2]</sup> or lipids<sup>[5,6]</sup> have been intensively investigated for various applications. For example, some of the membrane-recognition DNA has shown enhanced cellular uptake via a receptor-mediated mechanism or by increased membrane permeability.<sup>[15]</sup> However, current published data associated with membrane-anchored DNA focus exclusively on the effect of the hydrophobic moieties. As DNA is an important component of our micelles, we designed experiments to understand how DNA micelles with different sizes interact with cell membranes. To simplify the experiment, we first investigated the interaction using a model membrane. Briefly, 2  $\mu$ M DNA micelles were mixed with small unilamellar vesicles (SUVs, 200  $\mu$ M DSPC) in PBS buffer, and the pyrene fluorescence was monitored at different time intervals. Ratiometric fluorescence changes (excimer fluorescence decreases while monomer fluorescence increases) were observed for all four DNA micelles (SI, Fig. S6), indicating that fusion occurred between micelles and vesicles. This result suggests that the DNA micelles dissociate themselves and insert into the model membrane spontaneously. Interestingly, the sizes of DNA micelles greatly affect the fusion kinetics. Small micelles have faster fusion rate, while large DNA micelles show slow fluorescence response (SI, Fig. S6). A possible explanation is that large micelles have more densely charged coronas, which protect the lipid from exposure to phospholipid vesicles. It was also reported that exposure of the membrane recognition moiety is necessary for efficient cell internalization.<sup>[17]</sup>

Having established the fusion between DNA micelles and synthetic liposomes, we next investigated the affinity between the DNA-micelles and a plasma membrane. 200nM 3'-FAM-labeled DNA-micelles (lipo-n-FAM, same sequence as lipo-n) were incubated with cultured human T lymphoblast cell line from acute lymphoblastic leukemia (CCRF-CEM cells) for 1 hour. Both Confocal microscopy and flow cytometry were used to image and quantify the fluorescent profiles. FAM-20, a 20 mer DNA which lacks the lipid moiety, was used as a control. CEM cells treated with DNA-micelles were highly fluorescent when compared to those treated with the controls (Figure 4). To quantify the fluorescence, we used flow cytometry for a statistical analysis. Flow data revealed that CEM cells treated with DNA-micelles were 601 (lipo-5-FAM), 341 (lipo-10-FAM), 240 (lipo-20-FAM), and 85 (lipo-50-FAM) times more fluorescent than the population treated with control. Although the efficiency may be further optimized by varying many parameters of the internalization experiments, these results indicate that our DNA-micelles have strong affinity toward the plasma membrane. In addition, similar to the previous fusion data obtained by using DSPC vesicles, the fluorescence enhancements are size-dependent. Small micelles give larger fluorescence enhancement (lipo-5-FAM, 601 times, for example), while the enhancement decreases to 85 times when big micelles (lipo-50-FAM) were used. The flow cytometry data are in excellent agreement with the confocal imaging (Figure 4).

A higher magnification image reveals the cellular distribution of the DNA (Figure 5a). To get clear fluorescence images, we replaced the 3'-FAM with TAMRA because FAM is extremely pH sensitive. The fluorescence DNA was found to be uniformly distributed on the plasma membrane and also accumulated inside the cells. Next, we explored the cellular locations of the internalized DNA. Co-localization of our DNA-micelles via a better-characterized endocytic pathway, namely transferrin receptor (TfR)-mediated endocytosis,<sup>[18]</sup> was examined by confocal microscopy. As shown in Figure 5, the cell fluorescence after treatment with DNA-micelles was found to co-localize with Tf-containing endosomes, suggesting that the DNA accumulates in endosomes. It is known that amphiphilic molecules can avidly incorporate themselves in cellular plasma membranes and rapidly cycle between the plasma membrane and intracellular endosomes.<sup>[19]</sup> Thus, the



findings of fluorescence accumulation on membrane and in endosome, plus the fusion between DNA-micelles and vesicles, strongly suggest that our DNA -micelles undergo a similar endocytic cell uptake mechanism.

Amphiphilic molecules, such as SDS, exhibit dose-dependent toxicity to biological systems.<sup>[20]</sup> To examine the toxicity of the DNA-micelles, cellular viability was assessed by flow cytometry. Lipo-20 was incubated with CCRF-CEM cells at different concentrations, and the dead cells were determined by a PI staining assay. Under these conditions, virtually no cell death was observed, even at high micelle concentration (5 $\mu$ M DNA), thus showing no signs of cytotoxicity (SI, Fig. S7).

In our experiments, we did not observe fluorescence escape from endosomes. The fact that fluorescence can only be observed on cell membranes and endosomes might be explained by the strong hydrophobicity of the lipid molecule we used. Enrichment of lipophilic oligonucleotides on cell membrane and endosome might be explored for targeting specific receptors, for example, several categories of toll-like receptors (TLR3, TLR7, TLR8 and TLR9) are found primarily on endosomal membranes.<sup>[21]</sup> Thus, our DNA-micelles might then be used for delivery DNA/RNA or other targets which can specifically interact with toll-like receptors to enhance immunogenicity. On the other hand, a stable insertion of functional DNA (aptamer) onto cell surface can be applied for designing artificial cell membrane receptors. We are currently exploring this line of research.

## Conclusion

In summary, we have designed and constructed highly stable, well-defined oligonucleotide micelles; these micelles have a hydrophobic lipid core and a hydrophilic DNA corona. Preliminary data showed that the DNA-micelles showed a size-dependent affinity toward cell membranes and could be internalized by endocytosis. This design can be applied to any type of functional oligonucleotide (RNA, aptamer or DNAzyme),<sup>[22]</sup> making it attractive for the assembly of functionally controlled structures. In addition, the fact that the DNA-lipid can permeate a plasma membrane suggests that these micelles could serve as an artificial cell membrane receptor.<sup>[19,23]</sup> We believe that the monodispersed size, high stability, and size-dependent cell permeability of this class of micelles will find applications in nanobiotechnology, cell biology, and drug delivery.

## Experimental Section

### Materials

Unless otherwise stated, all solvents and chemicals were obtained from Sigma-Aldrich without further purification. HPLC was performed on a Varian Prostar system; UV/Vis was recorded by Varian Cary 100 spectrophotometer; fluorescence spectra were obtained on SPEX® FluoroLog® fluorometer; <sup>1</sup>H NMR and <sup>31</sup>PNMR were recorded on a Varian Mercury (300MHz) spectrometer using tetramethylsilane (TMS) as an internal standard; chemical shifts are reported in ppm ( $\delta$ ) referenced to TMS. Oligonucleotides were synthesized in 1.0 micromolar scale on an automated DNA synthesizer (ABI 3400, Applied Biosystems, Inc.). After cleavage and deprotection with aqueous ammonium hydroxide (55°C, 14 hours), the DNA was purified by reverse phase HPLC and quantified by UV spectrometer.

### DNA synthesis

All DNA sequences were synthesized by using the ABI 3400 synthesizer on 1.0 micromolar scale. Pyrene phosphoramidite was coupled by extended coupling time (900 seconds). Lipid phosphoramidite was dissolved in dichloromethane and was coupled by the so-called

syringe synthesis technique.<sup>5</sup> As an alternative, diacyllipid phosphoramidite could also be coupled using the DNA synthesizer. After the synthesis, the DNA was cleaved and deprotected from the CPG and purified by reverse phase HPLC using a C4 column (BioBasic-4, 200mm × 4.6mm, Thermo Scientific) with 100 mM triethylamine-acetic acid buffer (TEAA, pH 7.5) and acetonitrile (0–30 min, 10–100%) as an eluent (SI, Fig. S1).

Lipo-5: 5'-Lipo-Py-TTT TT -3'

Lipo-10: 5'-Lipo-Py-TTT TTT TTT T -3'

Lipo-20: 5'-Lipo-Py- AAA AAA AAT CAC AGA TGA GT -3'

Lipo-50: 5'-Lipo-Py- AAA AAA AAT CAC AGA TGA GTC TCT AAA AAG CCT  
AAA AAC ACG TGC GTA GA -3'.

### Agarose Gel Electrophoresis

Each DNA sample (1 µg) was analyzed by electrophoresis for about 90 min, under constant 75 V, through a 4% agarose gel in 1xTBE (Tris(hydroxymethyl)aminomethane (Tris, 89 mM), ethylene diamine tetraacetic acid (EDTA, 2 mM), and boric acid (89 mM), pH 8.0) buffer. The DNA bands were visualized by UV illumination (312 nm) and photographed by a digital camera.

### Critical Micelle Concentration Determination

Typically, amphiphilic DNA was diluted in series concentrations using PBS buffer (120 µL). An equal volume of acetone was added to the solutions so that the excimer fluorescence disappeared. The acetone was evaporated by a speed vacuum, and the volume of the solution became about 50 µL. The solutions were then diluted to 120 µL, and fluorescence spectrum was measured by a fluorometer. The critical micelle concentration was determined by the distinguishable pyrene excimer fluorescence of the corresponding DNA concentration.

### Micelle Characterization

AFM images were obtained using a Nanoscope IIIa (Digital Instruments) operated under tapping mode. A drop of DNA sample solution (2 µL) was spotted onto freshly cleaved mica (Ted Pella, Inc.) and left to adsorb to the surface for 30 seconds; then, 1xPBS buffer (50 µL) was placed onto the mica. Imaging was performed by tapping mode AFM under PBS buffer in a fluid cell, using NSC18/ALBS tips (Silicon cantilever, MikroMasch, Inc.) The tip-surface interaction was minimized by optimizing the scan set-point.

The particle sizes (diameters) and their distribution were measured by a ZetaPALS DLS detector (Brookhaven Instruments, Holtsville, NY, USA) at 25 °C. The scattering angle was fixed at 90°.

### CEM Cell Culture

CCRF-CEM cells (CCL-119 T-cell, human acute lymphoblastic leukemia) were obtained from ATCC (American Type Culture Association). CEM cells were grown in Dulbecco's modified Eagle's medium supplemented with 10% fetal bovine serum (Invitrogen) at 37 °C in 5% CO<sub>2</sub>. Cells (200 µL, 1×10<sup>6</sup> cells/mL) were cultured in a 96-well plate, incubated with DNA micelles (200 nM DNA), and imaged using scanning confocal microscopy.

### Flow cytometric assay for detection of dead cells

CEM Cells (200 µL, 1×10<sup>6</sup> cells/mL) were suspended in 1xPBS buffer and cultured in a 96-well plate. After incubation with DNA micelles (200 nM DNA) for 4 hours, cells were

washed twice with 1xPBS buffer and were cultured for an additional 48 h. The cells were stained with propidium iodide PI dye (PI; Invitrogen, Carlsbad, CA, 1  $\mu\text{g/mL}$ ) at room temperature for 20 min to test cell viability. Dead cells, which can accumulate the dye and show red fluorescence, were determined by a FACScan cytometer (Becton Dickinson Immunocytometry Systems, San Jose, CA).

### Preparation of Small Unilamellar Vesicles (SUVs)

Stock lipids (1,2-Distearoyl-sn-glycero-3-phosphocholine, DSPC) were dried from chloroform solution under nitrogen and then under vacuum overnight. The lipids were resuspended in a 1xPBS solution, pH 7.4, by vortex mixing. The lipid suspension was then passed through two stacked polycarbonate filters (100 nm) nineteen times in a mini-extruder (Avatilibids). The result is a suspension of small unilamellar vesicles containing a total of 1mM phospholipids in PBS buffer.

### Acknowledgments

We thank Prof. Chengde Mao for critical reading of the manuscript. We also thank Dr. Joseph Phillips, Dr. Yu-Fen Huang, and Dr. Wenqiang Tang for their helpful discussions and suggestions. This work is supported by NIH and DoD ONR grant.

### References

1. a) Hartgerink JD, Beniash E, Stupp SI. *Science*. 2001; 294:1684–1688. [PubMed: 11721046] b) Hartgerink JD, Beniash E, Stupp SI. *Proc Natl Acad Sci USA*. 2002; 99:5133–5238. [PubMed: 11929981] c) Lim Y, Lee E, Lee M. *Angew Chem Int Ed*. 2007; 46:9011–9014. d) Reches M, Gazit E. *Nature Nanotechnology*. 2006; 1:195–200.
2. a) Jeong JH, Park TG. *Bioconjugate Chem*. 2001; 12:917–923. b) Gosse C, Boutorine A, Aujard I, Chami M, Kononov A, Cogne-Laage E, Allemand JF, Li J, Jullien L. *J Phys Chem B*. 2004; 108:6485–6497. [PubMed: 18950138] c) Li Z, Zhang Y, Fullhart P, Mirkin CA. *Nano Lett*. 2004; 4:1055–1058. d) Safak M, Alemdaroglu FE, Li Y, Ergen E, Herrmann A. *Angew Chem Int Ed*. 2007; 19:1499–1505. e) Dentinger PM, Simmons BA, Cruz E, Sprague M. *Langmuir*. 2006; 22:2935–2937. [PubMed: 16548535] f) Alemdaroglu FE, Ding K, Berger R, Herrmann A. *Angew Chem Int Ed*. 2006; 45:4206–4210. g) Alemdaroglu EE, Alemdaroglu NC, Langguth P, Herrmann A. *Adv Mater*. 2008; 20:899–902.
3. Chan YM, Boxer SG. *Curr Opin Chem Biol*. 2007; 11:1–7.
4. a) Discher DE, Eisenberg A. *Science*. 2002; 297:967–973. [PubMed: 12169723] b) Allen C, Maysinger D, Eisenberg A. *Colloids Surf B*. 1999; 16:3–27. c) Torchilin VP, Lukyanov AN, Gao Z, Papahadjopoulos-Sternberg B. *Proc Natl Acad Sci USA*. 2003; 100:6039–6044. [PubMed: 12716967] d) O'Reilly RK, Hawker CJ, Wooley KL. *Chem Soc Rev*. 2006; 35:1068–1083. [PubMed: 17057836]
5. Storhoff JJ, Elghanian R, Mucic RC, Mirkin CA, Letsinger RL. *J Am Chem Soc*. 1999; 120:1959–1964.
6. Syntheses of amphiphilic DNA have been reported for antisense and membrane anchor applications, but very few of them studied their supramolecular assemblies. Examples include the following: Brush CK. Lipo-phosphoramidites. US Patent. 5,420,330. May 30.1995 Gold L, Janjic N, Schmidt P, Vargeese C. Vascular endothelial growth factor (VEGF) nucleic acid ligand complexes. US patent. 6,168,778. 2001 Ramirez F, Mandal SB, Marecek JF. *J Am Chem Soc*. 1982; 104:5483–5486. Shea RG, Marsters JC, Bischofberger N. *Nucleic Acids Res*. 1990; 18:3777–3783. [PubMed: 2165251] Chan YM, Lengerich BV, Boxer SG. *Biointerphases*. 2008; 3:FA17–FA21. [PubMed: 20408664] Kurz A, Bunge A, Windeck AK, Rost M, Flasche W, Arbuzova A, Strohbach D, Müller S, Liebscher J, Huster D, Herrmann AA. *Angew Chem Int Ed*. 2006; 45:4440–4444. Bunge A, Kurz A, Windeck AK, Korte T, Flasche W, Liebscher J, Herrmann A, Huster D. *Langmuir*. 2007; 23:4455–4464. [PubMed: 17367171] Borisenko GG, Zaitseva MA, Chuvilin AN, Pozmogova GE. *Nucleic Acids Res*. 2009; 37:e28. [PubMed: 19158188]



7. a) Park C, Lee IH, Song Y, Rhue M, Kim C. *Proc Natl Acad Sci USA*. 2006; 103:1199–1203. [PubMed: 16423900] b) Jones G, Vullev VI. *Org Lett*. 2001; 3:2457–2460. [PubMed: 11483034]
8. Conlon P, Yang CJ, Wu Y, Chen Y, Martinez K, Kim Y, Stevens N, Marti AA, Jockusch S, Turro NJ, Tan W. *J Am Chem Soc*. 2008; 130:336–342. [PubMed: 18078339]
9. Tummino PJ, Gafni A. *Biophys J*. 1993; 64:1580–1587. [PubMed: 8324192]
10. Smiddy MA, Martin JEGH, Kelly AL, Kruif CG, Huppertz T. *J Dairy Sci*. 2006; 89:1906–1914. [PubMed: 16702254]
11. Liu H, Chen Y, He Y, Ribbe AE, Mao C. *Angew Chem Int Ed*. 2006; 45:1942–1945.
12. Liang X, Mao G, Ng SKY. *Colloids Surf B*. 2004; 34:41–51.
13. No excimer fluorescence was observed when pyrene units were coupled at the midpoint and 3' terminus of the DNA sequence, which proves that there was no random entanglement between the DNA coronas. For other stretched polyelectrolyte aggregates, see Zhang LF, Eisenberg A. *Science*. 1995; 268:1728–1731. [PubMed: 17834990]
14. Lukyanov AN, Gao Z, Mazzola L, Torchilin VP. *Pharm Res*. 2002; 19:1424–1429. [PubMed: 12425458]
15. a) Letsinger RL, Zhang G, Sun DK, Ikeuchi T, Sarin PT. *Proc Natl Acad Sci USA*. 1989; 86:6553–6556. [PubMed: 2771942] b) Soutschek J, et al. *Nature*. 2004; 432:173–178. [PubMed: 15538359] c) Bijsterbosch MK, Rump ET, De Vruh RLA, Dorland RR, Veghel R, Tivel KL, Biessen EAL, Berkel TJC, Manoharan M. *Nucleic Acids Res*. 2000; 28:2717–2725. [PubMed: 10908328]
16. Skobridis K, Husken D, Nicklin P, Haner R. *ARKIVOC*. 2005:459–469.
17. Alemdaroglu FE, Alemdaroglu NC, Langguth P, Hermann A. *Macromol Rapid Commun*. 2008; 29:326–329.
18. Yang J, Chen H, Vlahov IR, Cheng J, Low PS. *Proc Natl Acad Sci USA*. 2006; 103:13872–13877. [PubMed: 16950881]
19. Peterson BR. *Org Biomol Chem*. 2005; 3:3607–3612. [PubMed: 16211095]
20. Meyers SR, Juhn FS, Grisct AP, Luman NR, Grinstaff MW. *J Am Chem Soc*. 2008; 130:14444–14445. [PubMed: 18842041]
21. Roach JC, Glusman G, Rowen L, Kaur A, Purcell MK, Smith KD, Hood LE, Aderem A. *Proc Nat Acad Sci USA*. 2005; 102:9577–9582. [PubMed: 15976025]
22. Lu Y, Liu J. *Curr Opin Biotech*. 2006; 17:580–588. [PubMed: 17056247]
23. Willis MC, Collins B, Zhang T, Green LS, Sebesta DP, Bell C, Kellogg E, Gill SC, Magallanez A, Knauer S, Bendele RA, Gill PS, Janjić N. *Bioconjugate Chem*. 1998; 9:573–582.

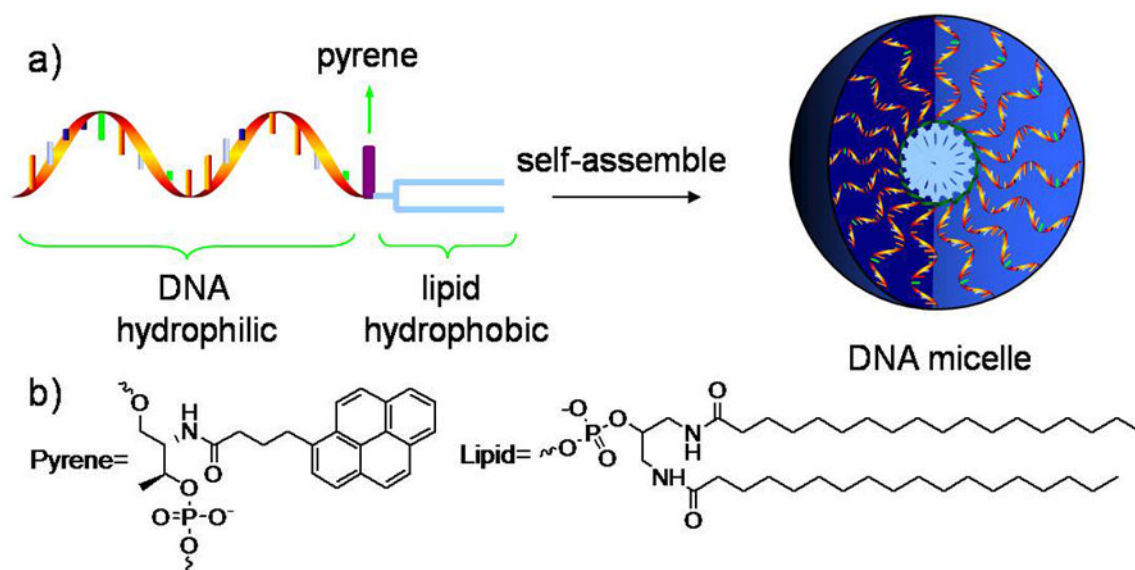


**Figure 1.** Schematic of the design and assembly of DNA micelles. (a) Oligonucleotide micelles contain a DNA corona, a pyrene unit (fluorescence reporter) and a lipid core. (b) Molecular structure of pyrene and lipid unit.

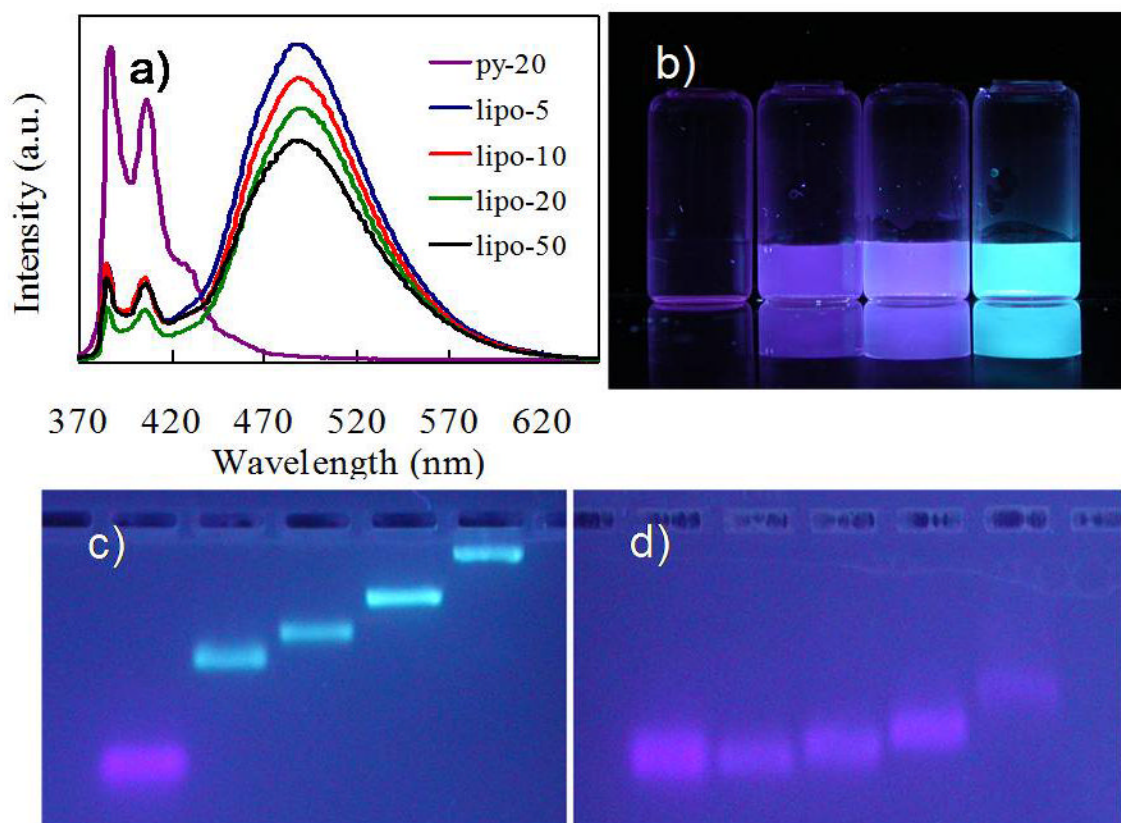


**Figure 2.**

Characterization of DNA-micelles by fluorescence and gel techniques. (a) Fluorescence spectra analysis of the assembled micelles. (b) Photographic image of micelle aggregation in different solvent systems. From left to right: ddH<sub>2</sub>O, Py-20 (same sequence as lipo-20, but no lipid was coupled) in PBS buffer, lipo-20 in PBS and acetone mixture (v/v 50:50) and lipo-20 in PBS buffer. Samples were illuminated by a UV transilluminator (312nm) and photographed by a digital camera. (c) and (d) 4% agarose gel analysis of amphiphilic DNA. From left to right: Py-20, lipo-5, lipo-10, lipo-20 and lipo-50. (c) Gel ran in 1xTBE buffer. (d) Gel ran in 1xTBE buffer containing 0.8% SDS.

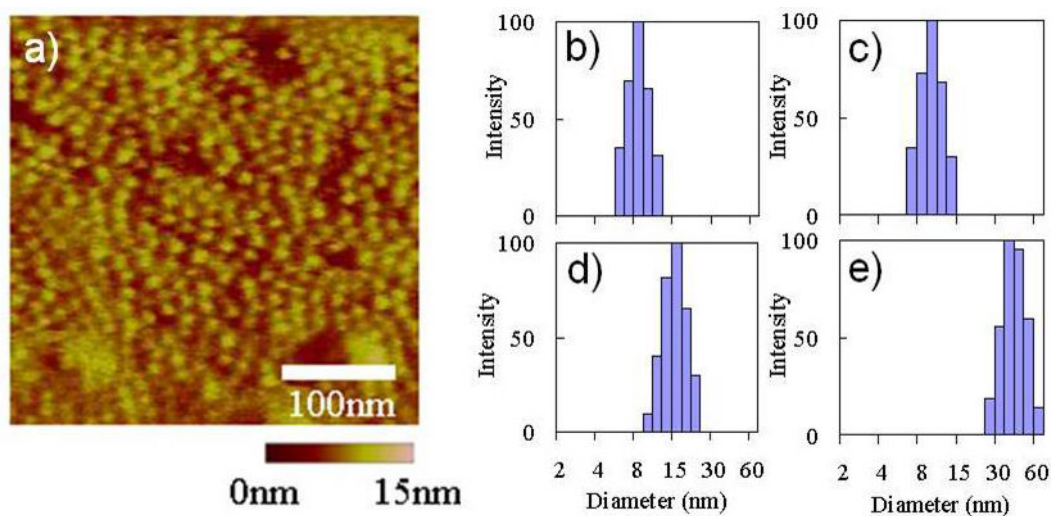


**Figure 3.**

Size analysis of DNA micelles. (a) AFM topography image of the self-assembled micelle (lipo-20) deposit on a mica surface. The sample was pipetted onto a freshly cleaved mica surface and imaged by tapping mode AFM in PBS buffer. Dynamic light scattering (DLS) data of lipo-5 (b), lipo-10 (c), lipo-20 (d) and lipo-50 (e).

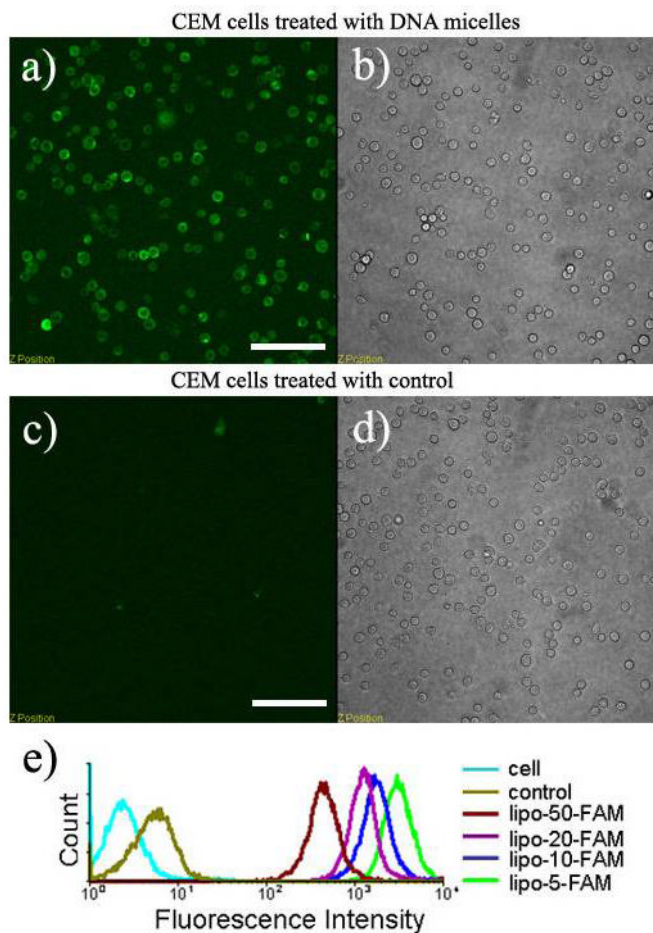


**Figure 4.**

Interactions between DNA-micelles and CEM cells. Cells were treated with 200nM DNA-micelles (top panels) and control (bottom panels) for 1 hour and subsequently examined by using confocal microscopy. (a) and (c) Fluorescence images; (b) and (d) transmitted images. (e) Flow cytometry data. The total mean fluorescence of the cell populations are 2.63 (untreated cells), 5.28 (FAM-20, control), 451 (lipo-50-FAM), 1270 (lipo-20-FAM), 1802 (lipo-10-FAM), and 3174 (lipo-5-FAM). (Scale bar: 50  $\mu$ m)



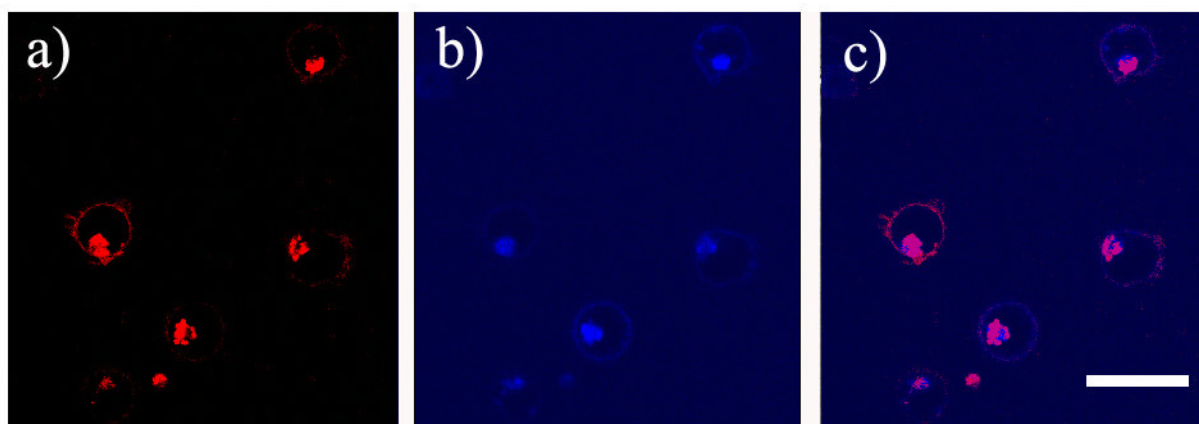


**Figure 5.**

Localization and distribution of the DNA-micelles in CEM cells. CEM cells were treated with TAMRA -labeled DNA-micelles (200 nM) and Tf-Alexa 633 (5 $\mu$ g/ml) for 30 minutes. After washing, cells were imaged for the TAMRA fragment (a) and transferrin Alexa 633 (b); (c) overlay of a and b. (Scale bar: 20  $\mu$ m)